J Geophys (1988) 62:109–118

Journal of Geophysics

Electromagnetic sounding experiments in the Schwarzwald central gneiss massif

B. Tezkan

Institut für Geophysik, Universität Göttingen, Herzberger Landstrasse 180, D-3400 Göttingen, Federal Republic of Germany

Abstract. Geomagnetic and telluric pulsations were observed at nine stations, partially at the same time, and at two sites with additional recordings of variations. They occupied a 20×30 km^2 area of high-grade metamorphism. There is a nearly perfect spatial uniformity of the magnetic variation field except for a small local anomaly attributable to the Rheingraben. The telluric field is highly polarized in a N47 $\pm$ 7W direction but with local differences in amplitude. In contrast, telluric phases are spatially uniform and, as a function of period, distinctly different for the N47W orientation of the telluric field (="*B*-polarisation") and the N43E orientation (="*E*-polarisation"). Telluric and magnetic observations are not explainable by one-dimensional (1-D) models for the Schwarzwald alone. Therefore a 2-D model is derived, comprising Schwarzwald and Rheingraben, which can account for the graben *Z* anomaly and the phase curves in both polarisations. An unscaled 1-D model is obtained from the telluric phases in *E*-polarisation and then a 2-D model for Schwarzwald and Rheingraben in *E*- and *B*-polarisation. This latter model allows the scaling of the 1-D Schwarzwald model and shows a thin conductive layer under the gneiss massif at a depth of 12 km with a conductance of 650 S.

Key words: Geomagnetic and telluric time variations – Magnetotellurics – Geomagnetic deep sounding – Electric conductivity structure – Rheingraben – Schwarzwald

Introduction

The Schwarzwald ("Black Forest") is one of the largest crystalline complexes of central Europe. It is 30 km wide and 100 km long, situated between the Rheingraben to the west and the Swabian Alps to the east. Two major crystalline rock types are exposed (Fig. 1): high-metamorphic and anatectic gneiss of probably Precambrian age and granitic rocks from Paleozoic plutonism during the Variscian orogenesis.

The electromagnetic sounding survey concentrated on the gneiss area which forms the central part of the Schwarzwald, known as „Hochschwarzwald". These are the survey stations: HTZ (Hinterzarten), BRE (Breitnau), NEU (Neukirch), STM (St. Märgen), LAN (Landeck), FRE (Freiamt), ELZ (Elzach), SNH (Schonach), TRI (Triberg), TIE (Tiefenbach), ENZ (Enzklösterle), GUE (Gütenbach). To study the influence of foliation of metamorphic rocks on the telluric field, to be expected in the gneiss area, two stations were placed on granitic rocks where foliation is absent: SNH and TRI, both on the so-called "Triberg Granite". Two stations (ENZ and LAN) were set up outside the exposed crystalline complex on Mesozoic Buntsandstein. But in either case the crystalline basement rocks are expected at shallow depth. Station LAN was the nearest one to the Rheingraben. This rift system is filled with unconsolidated young Mesozoic and Cenozoic sediments. Their resistivity is as low as 1 Ωm. To the west of the Rheingraben, which is at least 40 km wide, there is a second crystalline complex: the Vogesen ("Vosges").

At the east the Schwarzwald borders on Mesozoic sediments with resistivity not below 20 Ωm. Thus, along the eastern edge a less severe resistivity distribution was expected. The crystalline complex has been uplifted since late Cretaceous and early Tertiary, and afterwards deeply eroded. It shows strong signatures from the Variscian mountain building in the younger Paleozoics. The Variscian strike direction N45E is preserved in lineaments crossing the gneiss complex and also visible in gravimetric and static magnetic anomalies trending in about the same direction. The Rheingraben belongs to a continental-wide rift system with a mean strike of N15E in the portion which borders on the survey area. Subsidence began in the Tertiary and the sedimentary fill varies between 2500 m in the north and 1000 m in the south.

The purpose of the survey can be summarized as follows. From general experience it was to be expected that the telluric field on the exposed crystalline rock formation would be highly distorted, locally varying greatly in direction and amplitude over short distances. In the Bayerischer Wald („Bavarian Forest") for example, changes in amplitude by orders of magnitude were observed at stations 2.5 km apart, here under the influence of graphite-bearing schists close to the surface (Tezkan, 1984). Results of earlier MT soundings in the Schwarzwald at stations ENZ, TIE and HTZ have been presented by Richards et al. (1981). A new analysis of their data, now involving a rotation of coordinates, revealed surprisingly uniform telluric directions with a strong dominance of the field in a northwest direction. The general validity of this remarkable result was to be tested with a denser network of stations. Also available were MT results from the Rheingraben (Winter, 1973; Reitmayr, 1974) which allowed estimation of the graben sediment conductance (1000–1600 S) and of the resistivity of crust and mantle below. This information was essential

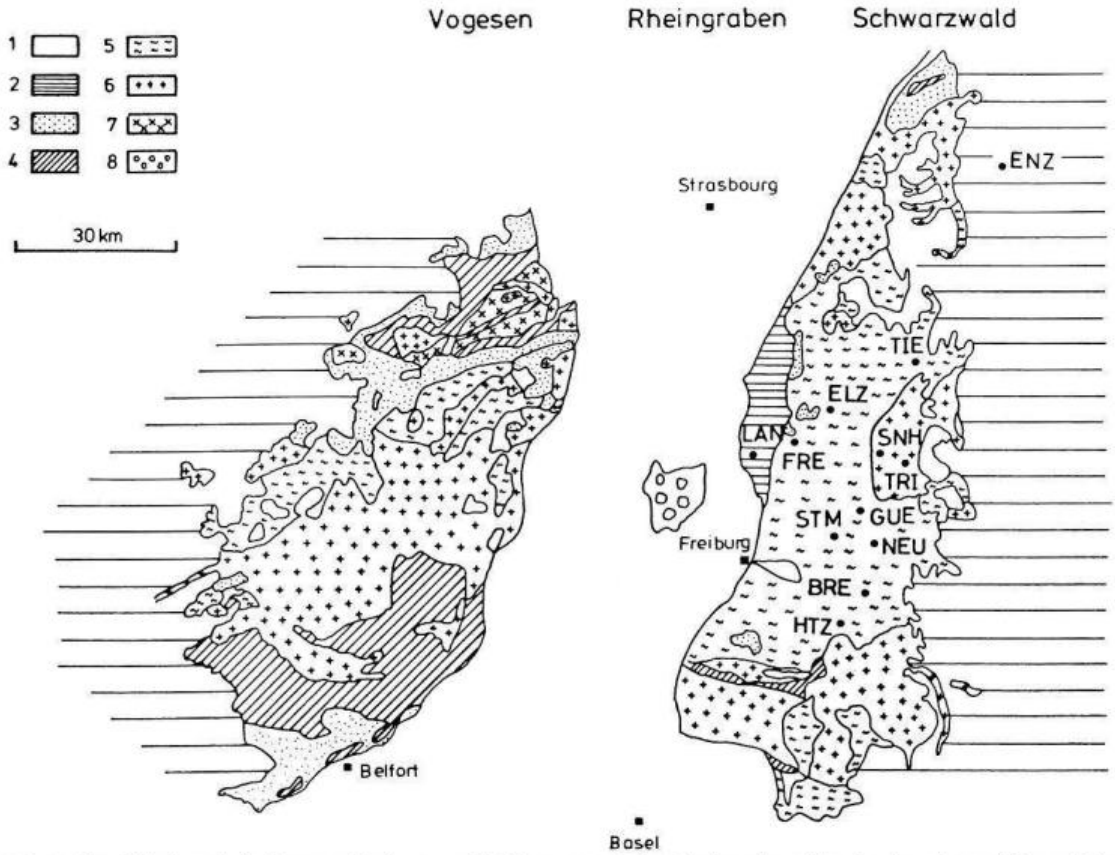

Fig. 1. Simplified geological map of Schwarzwald, Vogesen and the Rheingraben rift, showing the position of the survey stations. *1*, Cenozoic and Mesozoic graben sediments; *2*, Mesozoic sediments outside the graben; *3*, Permian sediments; *4*, Pre-Permian sediments; *5*, gneiss and migmatites; *6*, granite; *7*, granodiorites; *8*, Tertiary volcanics (Kaiserstuhl)

to estimate the induction effect of the Rheingraben sediments on the telluric and magnetic field in the survey area.

Teufel (1986) carried out a similar survey in the northern part of the Schwarzwald at about the same time, but with the inclusion of high frequencies. His results are in good agreement with the conclusion which can be drawn from the observations now to be presented.

Field survey and data analysis

The field survey was carried out with nine stations, recording simultaneously at four stations. They were equipped with induction coil magnetometers and *E*-field recording systems for the observation of pulsations. At one site a recording time of 2 or 3 weeks was needed to get responses of sufficient accuracy. At one station (GUE) it was impossible to record *E*-field pulsations because of industrial noise. Otherwise, for an industrial environment, low noise levels were observed. Variations were recorded for 8 weeks at two selected stations (TRI and NEU) equipped with fluxgate magnetometers. Altogether, a total of 20–30 h of about 100 time sections with strong activity for pulsations and 260–270 h of 70 time sections for variations were selected from the available records for spectral analysis.

The preliminary treatment of data in the time domain and the following analysis in the frequency domain were carried out with standard methods (Schmucker, 1978). Some of the essential results can be verified by visual inspection of the traces in Fig. 2. These time series of 9 min contain irregular oscillations in the period range between 10 and 100 s. The displayed records are not corrected for instrumental responses, but since response curves are similar for all sites direct comparison is possible.

Differences barely exist between the *H*- and *D*-pulsations of the magnetic field at different sites (*H*: north component, *D*: east component). The subsequent analysis confirmed this impression, i.e. the respective transfer functions for *H* and *D* show no significant anomalies. However, small differences in the *Z* component (vertical) can be recognized. Maximum *Z* amplitudes are observed at the most western stations, particularly at LAN (not shown in Fig. 2). The spectral analysis shows that the magnetic transfer functions for *Z* have a characteristic dependence on period attributable to the sediments of the Rheingraben. They produce a pronounced local *Z* anomaly near to the border of the Rheingraben, whereas the associated smooth anomaly of the horizontal component normal to the Rheingraben is too small to be recognizable in the Schwarzwald.

From the telluric pulsations in north (*EN*) and east (*EO*) directions, local differences in amplitudes are noticeable but not as severe as expected from experiences in the Bavarian Forest (Tezkan, 1984). The analysis shows that they can be very well correlated from station to station. Not visible in this figure is a pronounced telluric polarisation in a northwest direction. But this does not apply for station SNH on Triberg Granite. The *EN* and *EO* pulsations for

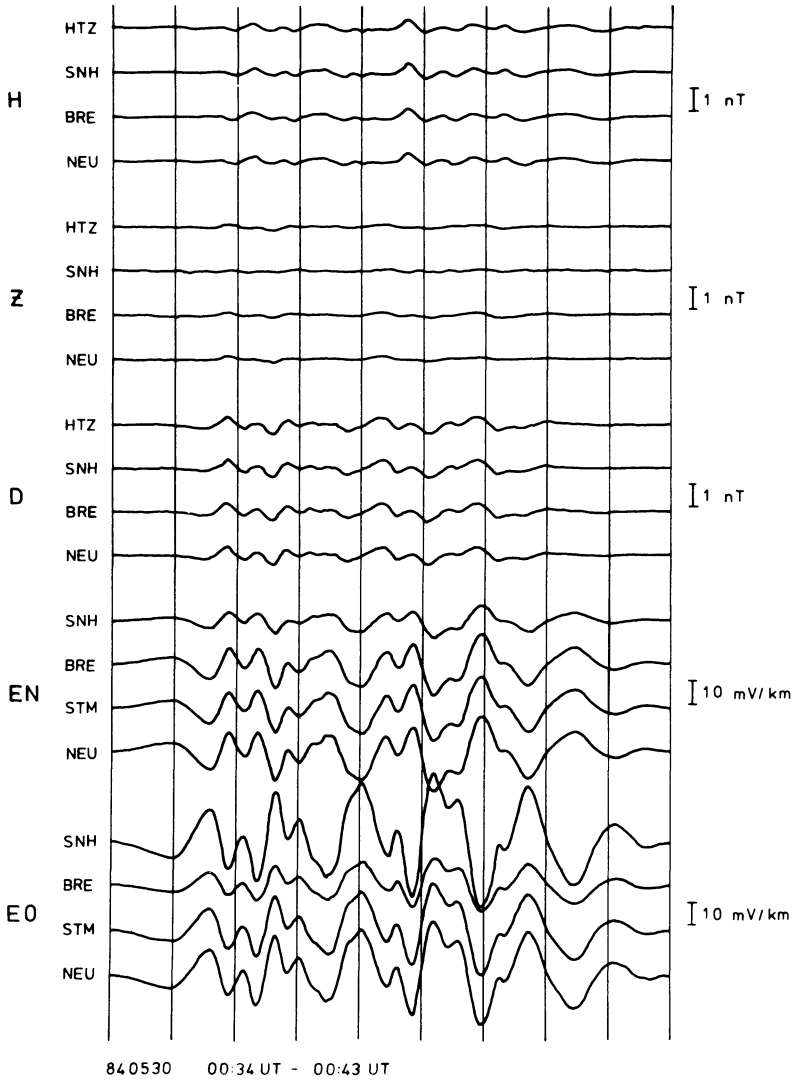

Fig. 2. Record sections of 9 min from four Schwarzwald stations. Nearly identical magnetic *H*, *D*, *Z* pulsations at all sites and similar telluric *EN* (north) and *EO* (east) pulsations at the gneiss stations BRE, NEU, STM. Station SNH on granite has different telluric amplitudes, reflecting different preferred coordinates

this station clearly differ from those at the other stations and the dominant telluric polarisation is different here, i.e. east-west.

For a fixed frequency and site, the complex Fourier coefficients of *Z*, *EN* and *EO* are connected with local *H* and *D* by the following set of transfer functions:

$$\begin{aligned} Z &= z_H H + z_D D + \delta Z \\ EN &= Z_{xx} H + Z_{xy} D + \delta EN \\ EO &= Z_{yx} H + Z_{yy} D + \delta EO \end{aligned} \qquad (1)$$

where δZ, δEN and δEO express the uncorrelated part in *Z*, *EN* and *EO*. The best-fitting transfer functions z_H, z_D ... will be considered those which produce minimum $<|\delta Z|^2>$. Averaging $<\cdots>$ is not only over neighbouring frequencies with spectral filters (Parzen filter), but also over assemblages of time sections. (Schmucker and Weidelt, 1975; Schmucker, 1978).

The coherence, in conjunction with the degree of freedom of the averaging procedure, establishes confidence limits for the transfer functions. They refer to an error probability of 32%. A squared coherency threshold was used in the analysis: 0.64 for magnetic transfer functions and 0.81 for electric transfer functions.

The spectral analysis was carried out in four overlapping frequency ranges for pulsations and in three overlapping frequency ranges for variations, with

$\Delta f = 0.1$ cpm and the central frequencies	0.1–0.8 cpm
0.2 cpm	0.2–3.0 cpm
0.5 cpm	0.5–3.0 cpm
1.0 cpm	1.0–8.0 cpm
$\Delta f = 0.1$ cph	0.2–0.8 cph
0.2 cph	0.6–2.0 cph
0.5 cph	1.0–5.0 cph.

The frequency unit is cpm = cycles per minute and cph = cycles per hour.

Electric and magnetic transfer functions for the Schwarzwald are presented and discussed in the following paragraphs. The derived linear relations in Eq. (1) can be explained as a function of frequency in such a way that the magnetic transfer functions z_H, z_D express the effect of lateral inhomogeneities of conductivity, i.e. the Rheingraben anomaly; whereas in the magnetotelluric impedance, the depth distribution of conductivity becomes visible only after considering its extreme directional dependence.

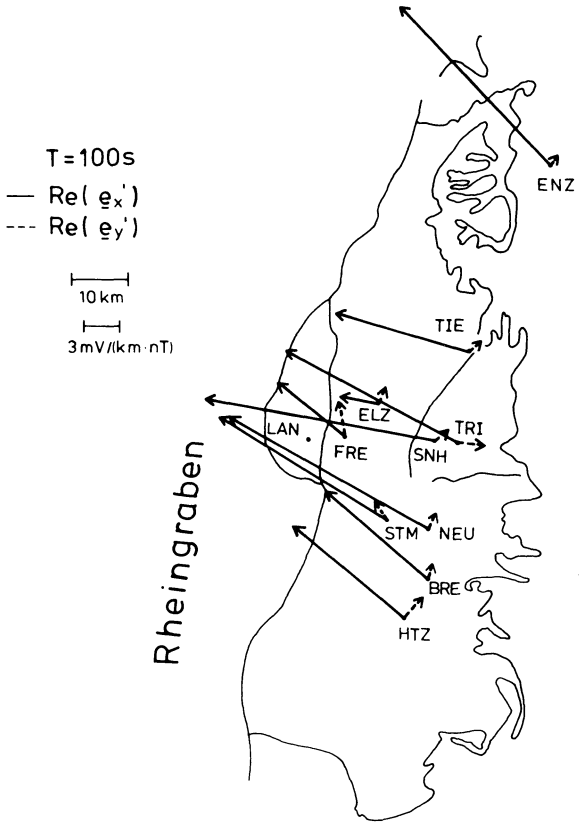

Fig. 3. Real part of the telluric vectors ($\mathbf{e}_{x'}$, $\mathbf{e}_{y'}$) in rotated preferred coordinates for all Schwarzwald stations except LAN (not included). It should be noted, however, that for stations SNH and TRI on the Triberg Granite, the chosen angle of rotation (43°) is not the optimum angle for the Swift criterion. A large but uniform directional dependence of the telluric field can be inferred: large-scale induced currents in a northwest direction, are 5–10 times stronger than those flowing in a northeast direction, isotropic conductivity assumed

Discussion of transfer functions

Magnetotellurics

For visual display, the tensor impedance Z for each site and frequency is represented by telluric vectors defined by:

$$\mathbf{e}_x = Z_{xx}\hat{\mathbf{x}} + Z_{yx}\hat{\mathbf{y}} \qquad (2)$$
$$\mathbf{e}_y = Z_{xy}\hat{\mathbf{x}} + Z_{yy}\hat{\mathbf{y}}$$

where $\hat{\mathbf{x}}$ and $\hat{\mathbf{y}}$ are unit vectors toward north and east. Assuming an isotropic conductivity distribution they indicate amplitude, phase and direction of the electric currents flowing in the subsurface for linearly polarized magnetic fields in the x and y direction. Swift's criterion (Swift, 1967) for optimal coordinates is used, in which $|Z_{xx} - Z_{yy}|$ is at a minimum. Tensor impedances are transferred to these new preferred coordinates (x', y'), rotated clockwise by angle α. Such transformations will emphasize existing symmetries in the conductivity structure and are useful if the rotation angle turns out to be fairly independent of frequency and location.

With the exception of the stations on the Triberger Granite (TRI, SNH) and the Rheingraben border station (LAN), rotation angles are about the same for all Schwarzwald stations and frequencies. Their rotation angle is 43°, averaged over all frequencies and stations, with a standard deviation of 7°. The impedances cited in the following refer exclusively to this rotated coordinate system.

Figure 3 shows the real part of the telluric vectors $\mathbf{e}_{x'}$ and $\mathbf{e}_{y'}$ for all Schwarzwald stations for a period of 100 s. They indicate a strong but uniform directional dependence of the telluric field. The regionally induced currents flow with maximum strength (for isotropic conductivity) through the Schwarzwald in a northwesterly direction and they are 5–10 times weaker in the perpendicular direction. Minor differences exist in strength and direction, but a rather uniform anisotropy parameter $A = |Z_{y'x'}|/|Z_{x'y'}|$ exists, large compared to unity.

Figure 4 shows telluric vectors over the entire period range for two selected Schwarzwald stations: a typical gneiss station, BRE, and the Rheingraben border station, LAN. Note that a different rotation angle $\alpha = 69°$ was used for LAN. All vectors are normalized to period $T_o = 100$ s, using the scaling factor $\sqrt{T/T_o}$ for a uniform half-space. This implies that all normalized vectors would have the same length and direction (normal to the magnetic field) if the subsurface structure were uniform.

As seen on the left, $\mathbf{e}_{x'}$ vectors point correctly in the y' direction, which is roughly northwest. The changing apparent resistivity and phase as a function of period is evident (see also Figs. 5 and 6). They are associated later with the B-polarisation of a 2-D structure where the phase begins and ends at 45° with a minimum phase of 35° at intermediate periods. The telluric $\mathbf{e}_{y'}$ vectors to the right are comparatively small and irregular. As shown later, the $Z_{x'y'}$ or x'-component of this vector, to be associated with the E-polarisation, contains the whole information about the conductivity-depth distribution. Also evident from Fig. 4 is the persistent large anisotropy with no indication of approaching unity at short periods.

Certain local differences in $Z_{y'x'}$, assigned to B-polarisation, cannot be overlooked. This is clear by comparing the neighbouring stations FRE and ELZ in Fig. 3. But in view of the anisotropy, an explanation of the $Z_{y'x'}$ variability with models will not be attempted. Instead, a general conclusion can be drawn from Fig. 3 and 4: the Schwarzwald crystalline complex is surprisingly homogeneous in its conductivity structure, but with a strongly directional-dependent impedance yielding an anisotropy of about ten.

Because of this dependence it is difficult to derive conceptions for the conductivity-depth distribution. This difficulty is demonstrated in Fig. 5 by displaying the apparent resistivity $\rho_{aij} (= \mu_o/\omega |Z_{ij}|^2)$ of the three stations TRI, BRE, LAN; a granite station, a gneiss and a border station. The ρ_a curves for both polarisations are orders of magnitude apart. Hence, a simple connection to the true deep resistivity is not evident. However, the ρ_a-curves of the three stations have remarkably similar dependences on period for the two polarisations. The 45° descent of ρ_a for $Z_{x'y'}$ (E-polarisation) between 10 and 50 s can be interpreted by a good conductor at an undetermined absolute depth. But, as demonstrated later, the Rheingraben Z-anomaly will provide an absolute scaling of this depth.

The phases ϕ of impedances $Z_{x'y'}$ and $Z_{y'x'}$ confirm the results obtained from the period dependence of ρ_a. They are presented in Fig. 6 and show clear differences for the two polarisations. The following discussion will be based on phases rather than the period dependence of ρ_a. There

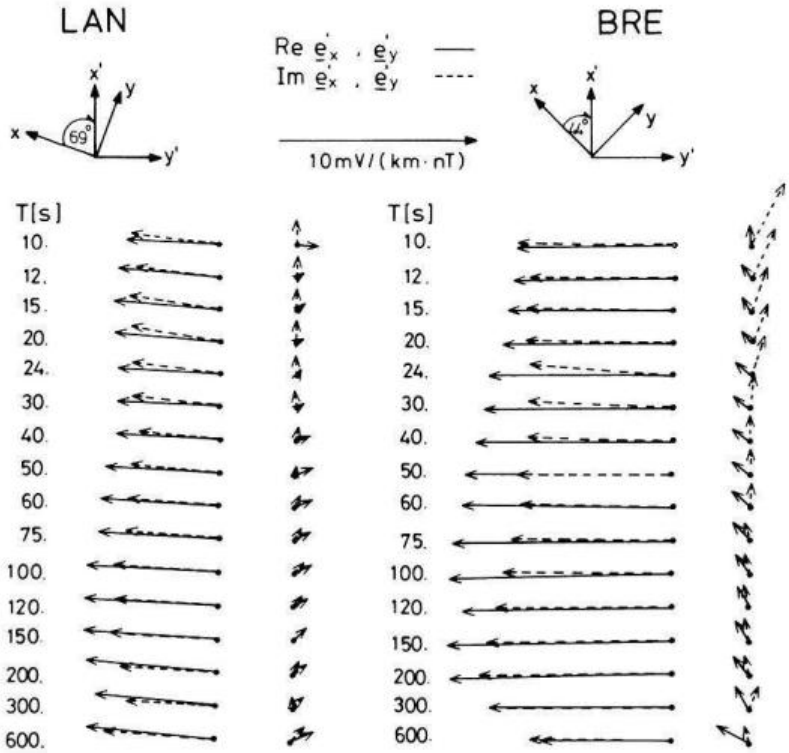

Fig. 4. Telluric vectors for two Schwarzwald stations in the period range 10–600 s, normalized to the period $T_o = 100$ s, with scaling factor $\sqrt{T/T_o}$ for a uniform half-space. Most conspicuous is the different lengths for the two polarisations. Small telluric $\mathbf{e}_{y'}$ vectors are associated with *E*-polarisation for a magnetic y'-polarisation and assumed to be close to the 1-D response of the Schwarzwald substratum. Their variable lengths with period reflect the changing conductivity with depth. Large and well-determined $\mathbf{e}_{x'}$ vectors indicate phases close to 45° with no direct bearing on the conductivity-depth distribution

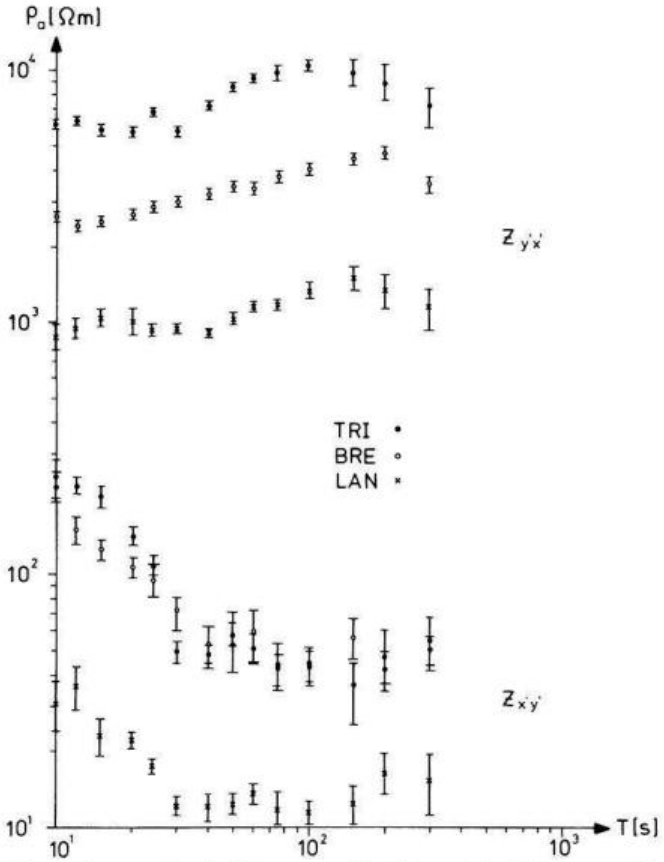

Fig. 5. Apparent resistivity curves for three typical Schwarzwald stations: *upper curves* for magnetic x'-polarisation (*B*) and *lower curves* for magnetic y'-polarisation (*E*) in rotated coordinates. The two sets of curves differ by one order of magnitude with systematically different period dependences. From the downward slope in the lower curves there is evidence for a good conductor beneath the Schwarzwald

Table 1. Apparent resistivities ρ_a(Ωm), phases ϕ (°) and anisotropy values *A* for $T = 60$ s

Station		*E*-polarisation ($Z_{x'y'}$)		*B*-polarisation ($Z_{y'x'}$)	
	A	ρ_a	ϕ	ρ_a	ϕ
BRE	0.96	60±14	59.6±6.8	3480±120	35.7±1.0
NEU	1.56	69±15	60.8±6.1	9360±210	36.3±0.6
STM[a]	1.36	16± 4	76.4±8.0	7630±340	35.1±1.2
SNH[c]	4.54	89±16	67.9±5.0	8340±210	35.6±0.7
LAN[b]	0.272	79± 7	50.2±2.4	1000± 40	37.4±1.2
FRE[b]	0.735	165±16	56.0±2.7	1650± 90	39.7±1.5
TRI[c]	2.12	100±14	56.0±3.9	880±220	36.2±0.7

[a] Only telluric observations, reference magnetic field is BRE
[b] Border stations
[c] Granite stations

is an ascent of the phase for *E*-polarisation from 70° to 80° between 10 and 15 s and then a drop to 45° which implies that a good conductor forms the lower boundary of the Schwarzwald crystalline complex as mentioned in the discussion of ρ_a curves. In contrast, the phases for *B*-polarisation stay close to 45° with a drop to 35° between 10 and 100 s. These characteristic phases are observed at all Schwarzwald stations and the difference in the two polarisations can be understood as an influence of the Rheingraben. Phases and apparent resistivities are tabulated in Table 1 for a period of 60 s. This table summarizes results from magnetotellurics as follows (Schmucker and Tezkan, 1985):

A) Amplitudes of *E* fields vary from station to station. The ρ_a curves of both polarisations lie far apart; for the *E*-polarisation below 100 Ωm and for the *B*-polarisation above 1000 Ωm.

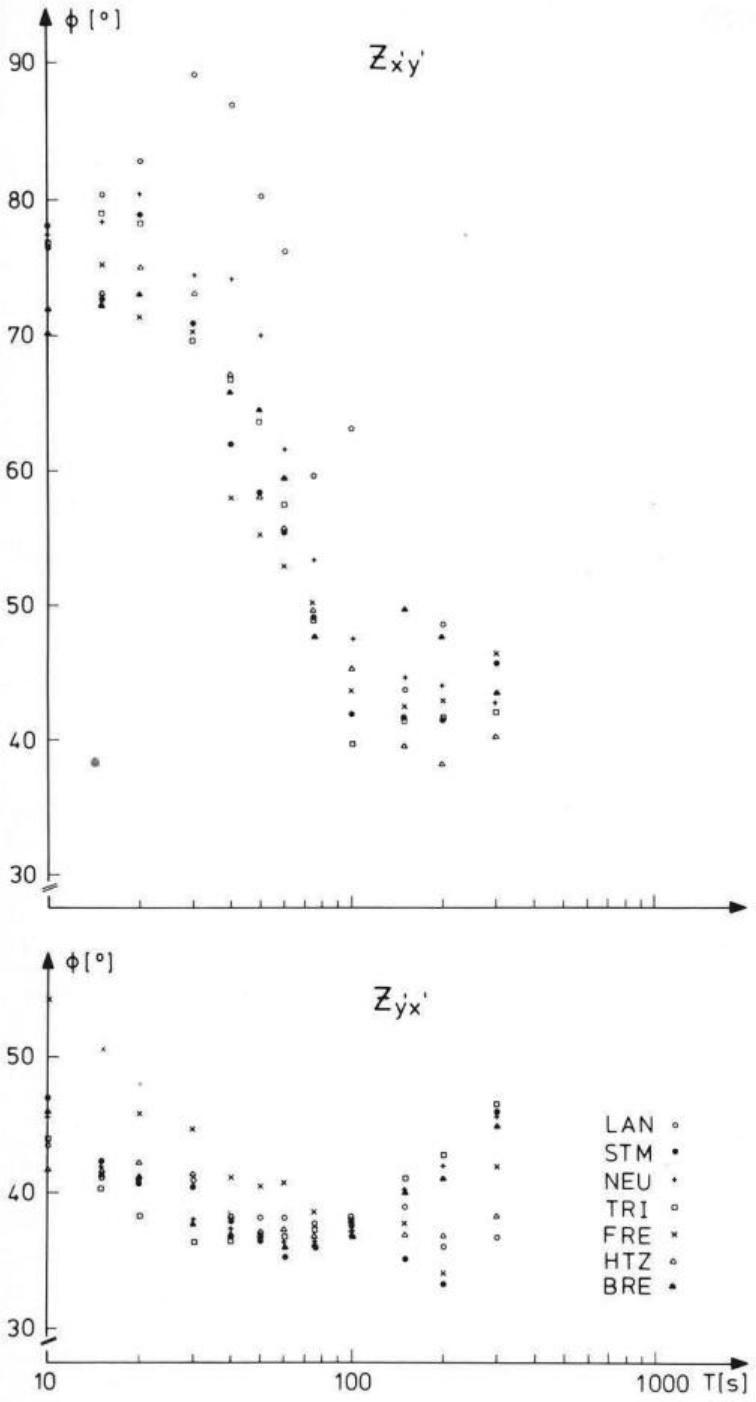

Fig. 6. Phase curves for all Schwarzwald stations in rotated coordinates. For easier visibility, no confidence limits are shown. Note their consistency for one polarisation and their systematic difference between *E*-($Z_{x'y'}$)- and *B*-($Z_{y'x'}$)-polarisation. The discrepancy in phase between the two polarisations can be understood as the 2-D effect of the Rheingraben sediments

B) Stable but different phases for the two polarisations; approximately 60° for the *E*-polarisation and 35° for the *B*-polarisation.

In addition, the impedance estimates are shown in Fig. 7, as a function of period, in the form of $\rho^*(z^*)$ curves. A typical gneiss station NEU is chosen, where long-period variations were also observed. ρ^* is a modified apparent resistivity considering the inductive effect of the top layers and defined by (Schmucker, 1979)

$$\rho^* = \rho_a \begin{cases} 2\cos^2\phi, & \phi \geqq 45° \\ 1/(2\sin^2\phi), & \phi \leqq 45° \end{cases} \qquad (3)$$

It is assigned as a substitute resistivity to a depth $z^* = \sqrt{\rho_a/\omega\mu_o}\cdot\sin\phi$. Such representations allow first estimates of the conductivity-depth distribution, and also test the consistency of the impedance for the 1-D condition in which z^* must monotonically increase with period. Figure 7 contains $\rho^*(z^*)$ depth sections lying far apart for *E*- and *B*-polarisations, as to be expected. Only the $\rho^*(z^*)$ curves for the *E*-polarisation ($Z_{x'y'}$) should be considered as a representation of the conductivity-depth distribution. The z^* depth values concentrate at 20 km with apparent resistivities below 10 Ωm for fast pulsations, reflecting the top of the conductor beneath the Schwarzwald crystalline com-

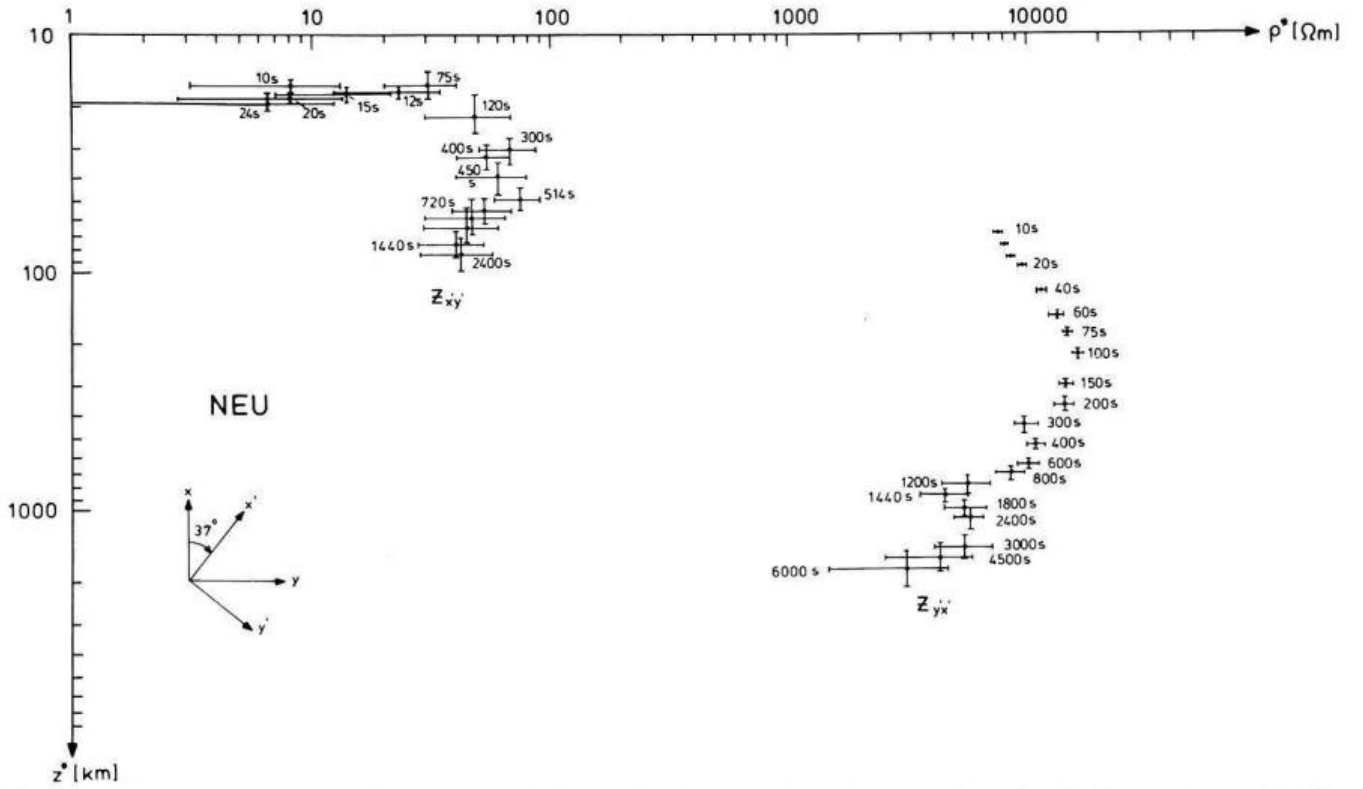

Fig. 7. $\rho^*(z^*)$ curves of E-$(Z_{x'y'})$- and B-$(Z_{y'x'})$-polarisation for the Schwarzwald station NEU. Only the $\rho^*(z^*)$ curve for E-polarisation should be considered as a representation of the true conductivity distribution beneath the Schwarzwald. Note that z^* values concentrate at 20 km with apparent resistivities below 10 Ωm between 10 and 75 s, reflecting the top of the crustal conductor beneath crystalline. Observe the ascent in ρ^* below that depth, indicating a transition to a normal mantle resistivity of 50 Ωm

plex. A strong ascent of apparent resistivity begins at 75 s with peak values of 70 Ωm for 300–500 s and a depth z^* of 40 km. From 700 s onward, there is a descent of apparent resistivities to 40 Ωm, reflecting the resistivity of the deeper layer of the upper mantle beneath Schwarzwald. But note that the quoted values $\rho^*(z^*)$ are still subject to scaling factors.

Geomagnetic depth sounding

The interpretation of the magnetic transfer functions concerns the anomalies of the vertical magnetic field variations because no visible anomaly in the horizontal field exists in the Schwarzwald, as discussed before.

Figure 8 shows a map representation of the transfer functions (z_H, z_D) in the form of induction arrows. With the notation of Eq. (1), the induction arrows are defined by the real and imaginary part of **u**

$$\mathbf{u} = z_H \cdot \hat{\mathbf{x}} + z_D \cdot \hat{\mathbf{y}}, \tag{4}$$

where $\hat{\mathbf{x}}$ and $\hat{\mathbf{y}}$ are unit vectors. Length and direction of these arrows are independent of the coordinate system and point away from the good conductor towards less-conducting zones. They are perpendicular to the strike of a 2-D anomaly. The closer a station is situated to a lateral contrast of conductivity, the larger is the anomalous Z and thus the length of **u**.

As seen in Fig. 8, the induction arrows of all stations point away from the Rheingraben as a good conductor. The largest arrow lengths are found at the border stations LAN and FRE, oriented perpendicular to the local eastern boundary of the Rheingraben. In all probability, the observed Z pulsations represent the graben effect and no substantial changes of conductivity are seen in the Schwarzwald crystalline complex itself, at least not in the analysed period interval. This applies especially to the good conductor beneath the Schwarzwald, which seems to have a regionally uniform depth and conductance.

A characteristic period dependence of the graben border anomaly is found. It can be inferred from the profile representations in Fig. 10, which also demonstrates the decrease of the graben anomaly with increasing distance from the Rheingraben of the four Schwarzwald stations LAN, FRE, SNH and TRI.

Interpretation of the transfer functions by models

Results of magnetotelluric and geomagnetic depth sounding contain different information about the conductivity distribution, as discussed earlier. Now, an attempt will be made to interpret them jointly with two-dimensional models.

However, the representation of impedance tensor elements in the form of telluric vectors shows that it will be difficult to find a model which is able to explain the large anisotropy as well as the locally very variable apparent resistivity. It can be assumed that surficial well-conducting veins in a poorly conducting environment do not change the magnetic variation field at sufficiently long periods. On the other hand, the amplitudes of the electric field can be severely affected, whereas their phases remain unchanged.

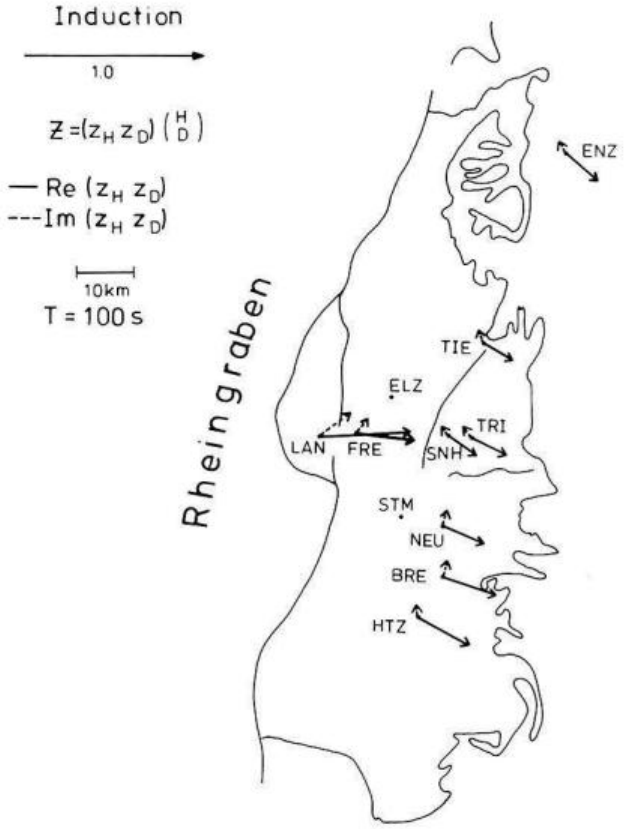

Fig. 8. Map representation of induction arrows for all Schwarzwald stations for a period of 100 s. Maximum Z values are observed at western border stations and all arrows point away from the Rheingraben as a good conductor. In all probability, the observed Z pulsations represent the graben effect and no substantial lateral changes of conductivity are seen in the Schwarzwald crystalline complex itself

For this reason, we try to calculate a 2-D model which explains the Rheingraben Z anomaly as well as the period dependence of the phase curves for the off-diagonal impedance elements $Z_{x'y'}$ and $Z_{y'x'}$. These are the data which can be reproduced by models.

First of all an unscaled 1-D model, which is not shown here, is derived from the telluric phases in E-polarisation. It is used as a starting model for the 2-D model calculations. The conductance of the Rheingraben sedimentary filling and the deeper conductivity distribution beneath it are adopted from Winter (1973) and Reitmayr (1974). Further north of the investigated area, Winter quoted 2000 S (S = Siemens) for a sedimentary thickness of 2 km. In the model, a value of 1500 S is chosen because of the southwest decrease of the sedimentary thickness in the Rheingraben.

Before going into details, a fundamental difficulty must be mentioned. The calculated magnetic and electric transfer functions do not refer to the same coordinates: the Rheingraben in a N15E direction is chosen as the x'' strike direction of the 2-D model, with y'' as the direction of the model cross-section. The calculated magnetic Z anomaly for this cross section is compared directly with the observed transfer functions of Z. The model impedances $Z_{x''y''}$ and $Z_{y''x''}$, however, are compared with the observed impedances $Z_{x'y'}$ and $Z_{y'x'}$, referring to coordinates rotated by 43° from north, as determined by the Swift criterion. The discrepancy expresses the unavoidable deficiency of any interpretation by two-dimensional models. As discussed before, the (x', y') coordinates are optimal coordinates for the Schwarzwald impedances. This means that the coordinates for the Z anomaly and the impedances differ by 28°. The amplitudes of the electric field, i.e. the apparent resistivities derived by them, will remain unconsidered. Nevertheless, the model will explain those for E-polarisation, at least approximately.

The chosen 2-D model is shown in Fig. 9 with the coordinate system used for the magnetic and electric transfer functions. The observed border anomaly of Z and the phases of the off-diagonal elements of the impedance tensor are compared in Figs. 10 and 11 with model values obtained from the 2-D model in Fig. 9. $z_{D''}$ is the magnetic transfer function projected to the profile direction. The period dependence of the phase curves is critical for the modelling because of the regional uniformity of the phase for a fixed period.

The Rheingraben model above cannot explain the observed telluric graben anomaly alone; in particular, not in its phases. However, a well-fitting model can be obtained by adding a good crustal conductor beneath the Schwarzwald. Its depth and conductance can now be given by a joint interpretation of the graben anomaly in Z and the telluric phases.

The 2-D model cross-section in Fig. 9 for the Schwarzwald and Rheingraben successfully explains the local Z variations and the large offset between the phase curves of both polarisations. Ultimately, the sediments of the Rheingraben are the cause of the offset of the phase curves, but the conductivity structure beneath the Schwarzwald determines their course. The 2-D model now allows the scaling of the 1-D Schwarzwald model with the following results:

1) To a depth of 12 km, the Schwarzwald is poorly conducting (>200 Ωm) with no resolvable structure in the investigated period range.

2) Below that depth a thin conductor appears, underlain by a less-conducting deep crust (1000 Ωm) over a well-conducting half-space at 40 km (15 Ωm).

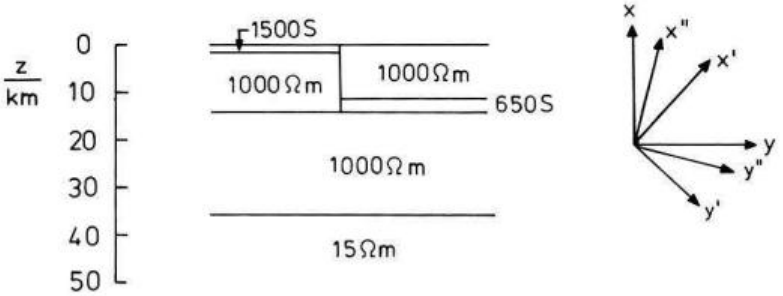

Fig. 9. 2-D model for the Rheingraben sediment to the *left* and the Schwarzwald crystalline complex to the *right*. The model is symmetric about the graben centre with a total graben width of 32 km. (x, y), geographic coordinates; (x'', y''), model coordinates used for a comparison with Z-transfer functions; (x', y'), optimal coordinates for the telluric field in the Schwarzwald, used for a comparison with the telluric transfer functions

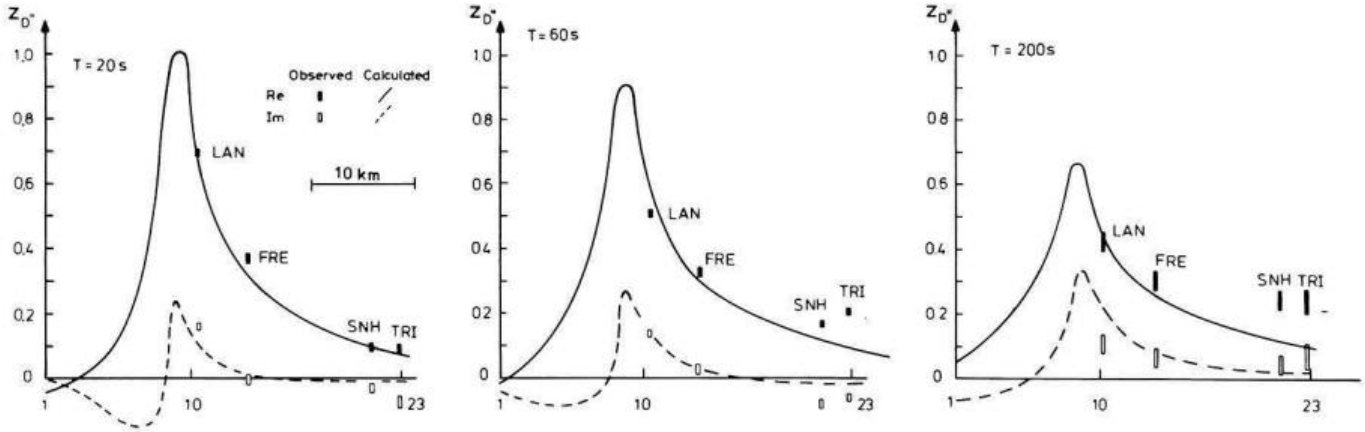

Fig. 10. In-phase and out-of-phase graben anomaly in Z, for the model in Fig. 9, as a function of distance from the graben centre. Observed and calculated transfer functions are compared for three periods. The indicated confidence limits refer to an error probability of 32%

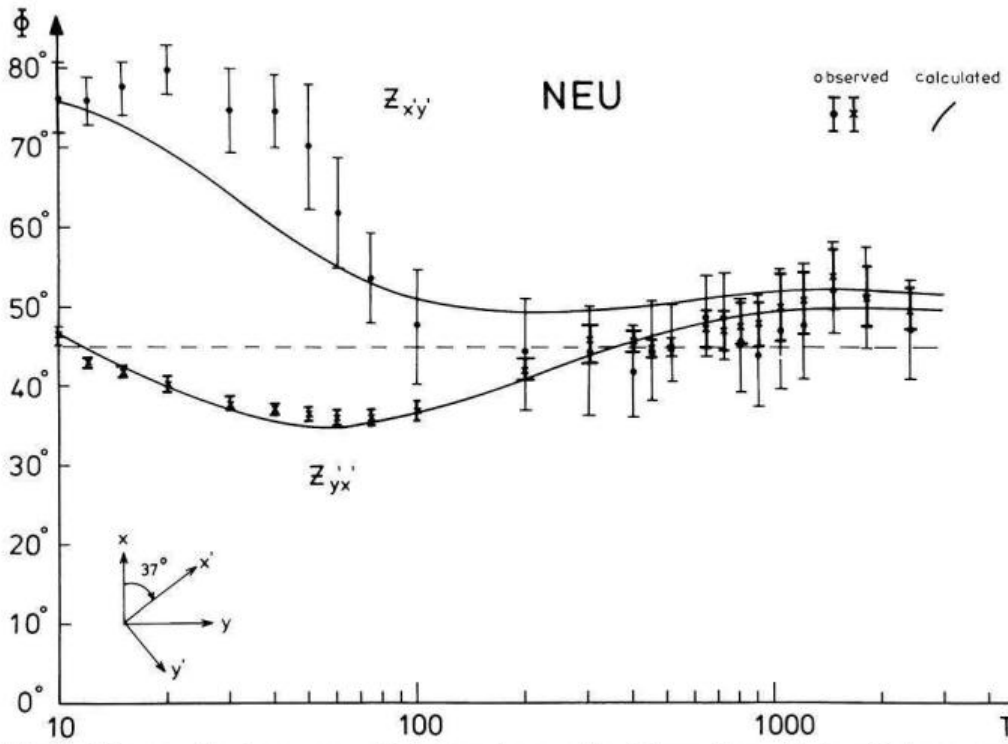

Fig. 11. Schwarzwald phase curves of the impedance, with their confidence limits referring to an error probability of 32%, for *E*- and *B*-polarisation for the model in Fig. 9 at 40 km distance from the graben centre. Calculated phases for periods from 10 to 3600 s are compared with empirical phases for gneiss station NEU at that distance. Note that on the Schwarzwald side, calculated and observed phases vary little with distance from the graben centre. Therefore, a comparable fit applies to all Schwarzwald stations

Numerical model studies show that some variations of the good conductor under the Schwarzwald are allowed, even though without this layer no satisfying fit can be obtained for Z variations as well as for the phases of the impedance. The best fit is obtained for a thin conductor at a depth of 12 km with a conductance of 650 S. The resistivity of this layer must be below 10 Ωm, corresponding to the ρ^* minimum in Fig. 7. A thorough investigation of acceptable models can be found in the discussion of observations in the northern Schwarzwald by Teufel (1986), who comes to similar conclusions.

Conclusion

The magnetic and electric transfer functions discussed can be considered as complete and conclusive. However, their interpretation with two-dimensional models is to be regarded as preliminary, in particular because calculated magnetic and electric transfer functions do not refer to the same coordinates when compared with observations.

Allowing for these principal difficulties, a two-dimensional conductivity distribution for the Schwarzwald was successfully derived:

A) The 2-D model of Fig. 9 explains the Z anomaly and the phases of the impedance in E- and B-polarisation.

B) The 2-D model calculations confirm the existence of a thin conductive layer under the Schwarzwald crystalline complex. The depth of this layer is at least 12 km and at most 18 km. The thickness of it cannot be resolved, but its conductance can be estimated to be 650 S.

C) The large anisotropy of the impedance and the variable apparent resistivities from station to station are not explained.

Acknowledgements: I wish to thank Prof. U. Schmucker for many stimulating discussions and for kindly reading the manuscript.

References

Reitmayr, G.: Elektromagnetische Induktion im Erdinnern, studiert am Rheingraben. Diss. Fak. f. Geowissenschaften der Ludwig-Maximilians-Universität München, 1974

Richards, M.L., Schmucker, U., Steveling, E., Watermann, J.: Erdmagnetische und magnetotellurische Sondierungen im Gebiet des mitteleuropäischen Riftsystem. Forschungsbericht T81-III, Bundesministerium für Forschung und Technologie, Bonn, 1981

Schmucker, U.: Auswertungsverfahren Göttingen. Protokoll Kolloquium Elektromagnetische Tiefenforschung. Neustadt/Weinstraße, 163–188, 1978

Schmucker, U.: Erdmagnetische Variationen und die elektrische Leitfähigkeit in tieferen Schichten der Erde. Sitzungsberichte und Mitteilungen der Braunschweigischen Wissenschaftlichen Gesellschaft. Sonderheft 4, Goltze Verlag, Göttingen, 45–102, 1979

Schmucker, U., Weidelt, P.: Electromagnetic induction in the Earth. Lecture notes, Aarhus, 1975

Schmucker, U., Tezkan, B.: Erdmagnetische und tellurische Untersuchungen im Schwarzwald. Bericht zum Unterantrag der Univ. Karlsruhe zum BMFT Förderungsvorhaben R683146, Inst. f. Geophysik, Univ. Göttingen, 1985

Swift, C.M.: A magnetotelluric investigation of an electrical conductivity anomaly in South Western United States. Ph.D. Thesis, M.I.T., Cambridge, Mass., 1967

Teufel, U.: Die Verteilung der elektrischen Leitfähigkeit in der Erdkruste unter dem Schwarzwald, ein Beispiel für Möglichkeiten und Grenzen der Interpretation von Audio-Magnetotellurik, Magnetotellurik, Erdmagnetischer Tiefensondierung. Diss. Fak. f. Geowissenschaften der Ludwig-Maximilians-Universität München, 1986

Tezkan, B.: Einfluß von Graphitgängen auf EM-Sondierungen mit Pulsationen im südöstlichen Bayerischen Wald. Protokoll Kolloquium Elektromagnetische Tiefenforschung, Grafrath, 145–152, 1984

Tezkan, B.: Erdmagnetische und magnetotellurische Untersuchungen auf den hochohmigen Kristallinstrukturen des Hochschwarzwaldes und des Bayerischen Waldes bei Passau. Diss. Math.-Nat. Fak., Univ. Göttingen, 1986

Winter, R.: Der Oberrheingraben als Anomalie der elektrischen Leitfähigkeit, untersucht mit Methoden der erdmagnetischen Tiefensondierung. Diss. Math.-Nat.Fak., Univ. Göttingen, 1973

Received March 6, 1987; revised July 10, 1987
Accepted August 7, 1987